

Elastic modulus measurement of the rod-shaped object based on image processing

Guoqiang Chen^a, Shaobin Lv, Xiaofeng Li, ZhiFei Yang and Ruidong Xu

School of Mechanical and Power Engineering, Henan Polytechnic University, Jiaozuo,454003, China

Abstract. Aiming at the problem of the method that demands a high accuracy of the equipment with a high price and low generality in measuring the elastic modulus by using the direct method, a device and a method are proposed to measure the elastic modulus of the rod-shaped object based on image processing. The image of the rod-shaped object is gotten using the proposed measurement device. The coordinates of the point on the contour line and the centroid of the cross-section of the rod-shaped object are extracted by using the object image with loading and no-loading respectively. The elastic modulus is computed by using the deflection difference formula. Finally an example is given to verify the feasibility and effectiveness of the device and method that lay a solid foundation for future study of the rod-shaped object elastic modulus measurement.

1 Introduction

The material elastic modulus is a key characteristic parameter that describes the ability to resist elastic deformation within the elastic limit^[1-2]. The elastic modulus is an important mechanical parameter in engineering technology^[3-8].

There are many existing measurement methods to the elastic modulus. Chen Cheng et al proposed the design of a measuring instrument for the elastic modulus of the metal wire based on a linear CCD^[9]. Lwanage Hiroshi et al introduced an equipment for the measurement of high temperature elastic modulus^[10]. Xu Jia-bin and others proposed the bending resonance method to measure the Young's modulus of the material^[11]. Christophe Auvray et al evaluated the Elastic modulus of claystone by nano-/micro-indentation tests and meso-compression tests^[12]. LI Ming-xiang proposed the measurement of Young's modulus of materials by laser interferometry based on the principle of double beam interference^[13]. Chiu Chin-chen et al developed relationships for determining the in-plane elastic modulus of a coating by two experimental techniques of dynamic resonance and static bend^[14]. Niu Lian-ping proposed a new improvement method for the problem of measuring the elastic modulus of steel wire by stretching^[15]. If the elastomer is exposed to the external force, it is difficult to measure the strain and stress quickly and accurately. Because there is not a consistent one-to-one match between deflection values and the force the rod-shaped object receives, the elastic modulus can be determined indirectly. Therefore, a device and a method are proposed to measure the elastic modulus of the rod-shaped object with the advantages of

simple operation, low equipment cost, high versatility and high measuring accuracy. The device and the method solve effectively the problem of measuring the elastic modulus of the rod-shaped object.

This paper is organized as follows. In Section 2, the device is presented for measurement the material elastic modulus. Section 3 describes the measurement step and method. An example is given to verify the feasibility and effectiveness of the device and method in Section 4. Section 5 concludes this paper.

2 Principle of the measurement device

The proposed measurement device consists of a monochrome board, a calibration block, a bracket mechanism, a computer, an image acquisition card, a data acquisition card, a loading device, a camera, and so on, as shown in Fig. 1. The camera is calibrated by using the calibration block. The effective length of the rod-shaped object is determined by adjusting the position of the mobile bracket on the base rail of the bracket mechanism. The rod-shaped object is placed in the upper fixed bracket and the mobile bracket in the upper groove. The loading device is placed on the loading rack. The position of the loading rack on the rail of the base can be adjusted. A loading force is applied by the loading device at the intermediate position of the effective length of the rod-shaped object. The rod-shaped object pictures are acquired for loading and no-loading, and the camera is controlled

*Corresponding author: ^a jz97cgq@sina.com

by a computer. The deformation images of the rod-shaped object are obtained and saved under different loading condition. The camera focal length and the distance from the camera to the rod-shaped object remain unchanged for taking the images. The images are processed using binarization, interference elimination, dilation, erosion, contour extraction, and so on.

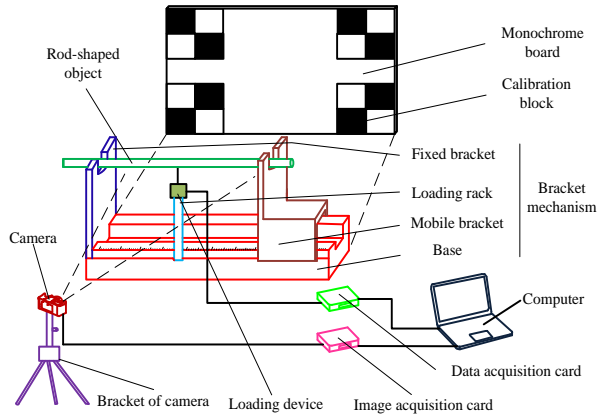


Figure. 1. The measurement device of the elastic modulus

3 Measurement steps and methods

The elastic modulus measurement method can be expressed as follows.

- Step1: The camera calibration block is calibrated.
- Step2: The images of the rod-shaped object are taken and the corresponding images are processed.
- Step3: The coordinates of the contour points are extracted on the upper and lower contours of the rod-shaped object with loading and no-loading respectively.
- Step4: The coordinates of the cross-sectional centroid of the rod-shaped object and the deflection difference between loading and no-loading are computed.
- Step5: The elastic modulus is obtained by using the deflection difference expression.

The coordinate system is shown in Fig. 2. The coordinates of the upper and lower contour points of the rod-shaped object are obtained by using the image processing technology. The contour points are extracted from left to right along the effective length of the rod-shaped object. The variables $x_1, x_2, x_3, \dots, x_N, x_{N+1}, x_{N+2}, x_{N+3}, \dots, x_{2N}$ are the abscissa values of the contour points, and N is an integer not less than 11.

The upper contour is marked as LRU (that consists of the left half LU and the right half RU), and the lower contour is marked as LRL (that consists of the left half LL and the right half RL). The curve LRC (that consists of the left half LC and the right half RC)

stands for the centroid of each cross-section along the length of the rod-shaped object.

Three algorithms are proposed to find the elastic modulus of the rod-shaped object.

Algorithm 1: The upper contour LU function $F_{LRU1}(x)$ and the lower contour LL function $F_{LRL1}(x)$ under no-loading condition can be fitted and expressed as

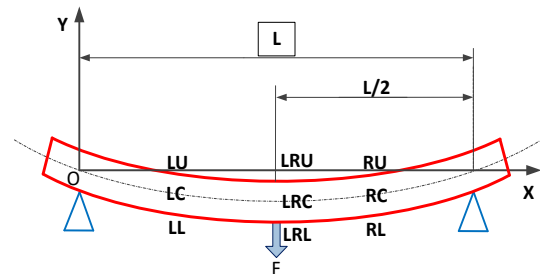


Figure. 2. The coordinate system

$$F_{LRU1}(x) = \sum_{k=0}^4 m_k x^k \quad (1)$$

$$F_{LRL1}(x) = \sum_{k=0}^4 n_k x^k \quad (2)$$

where m_k and n_k are the coefficients of the fitted functions.

The upper contour LRU function $F_{LRU2}(x)$ and the lower contour LRL function $F_{LRL2}(x)$ under loading condition can be fitted and expressed as

$$F_{LRU2}(x) = \sum_{k=0}^4 r_k x^k \quad (3)$$

$$F_{LRL2}(x) = \sum_{k=0}^4 l_k x^k \quad (4)$$

where r_k and l_k are the coefficients of the fitted functions.

The curve LRC under no-loading condition can be expressed as

$$F_{LRC1}(x) = \frac{F_{LRU1}(x) + F_{LRL1}(x)}{2} \quad (5)$$

The curve LRC under loading condition can be expressed as

$$F_{LRC2}(x) = \frac{F_{LRU2}(x) + F_{LRL2}(x)}{2} \quad (6)$$

The deflection difference $w_1, w_2, w_3, \dots, w_N, w_{N+1}, w_{N+2}, w_{N+3}, \dots, w_{2N}$ for each $x_1, x_2, x_3, \dots, x_N, x_{N+1}, x_{N+2}, x_{N+3}, \dots, x_{2N}$ can be obtained using $F_{LRC1}(x)$ and $F_{LRC2}(x)$ between loading and no-loading conditions.

$$w_z(x_z) = F_{LRC2}(x_z) - F_{LRC1}(x_z) \quad (z=1, 2, \dots, N, N+1, N+2, \dots, 2N) \quad (7)$$

If the both ends of the rod-shaped object are supported, the deflection curve can be expressed as^[16]

$$w_1(x) = -\frac{qx}{24EI}(L^3 - 2Lx^2 + x^3) \quad (8)$$

where q is the linear density of the rod-shaped object, L is the effective length of the rod-shaped object, and I is cross-section moment of inertia of the rod-shaped object.

$$w_2(x) = \begin{cases} -\frac{qx}{24EI}(L^3 - 2Lx^2 + x^3) - \frac{Fx}{48EI}(3L^2 - 4x^2) & 0 \leq x \leq \frac{L}{2} \\ -\frac{qx}{24EI}(L^3 - 2Lx^2 + x^3) + \frac{Fx-FL}{48EI}(-L^2 + 8Lx - 4x^2) & \frac{L}{2} < x \leq L \end{cases} \quad (10)$$

where F is the force in the middle of the effective length of the rod-shaped object, as shown in Fig. 2.

And the corresponding theoretical deflection difference can be expressed as

$$w(x) = w_2(x) - w_1(x) = \begin{cases} \frac{Fx}{48EI}(4x^2 - 3L^2) & 0 \leq x \leq \frac{L}{2} \\ \frac{Fx-FL}{48EI}(-L^2 + 8Lx - 4x^2) & \frac{L}{2} < x \leq L \end{cases} \quad (11)$$

Based on Equations (1) to (11), $2N$ elastic modulus $E_1, E_2, E_3, \dots, E_N, E_{N+1}, E_{N+2}, E_{N+3}, \dots, E_{2N}$ can be gotten corresponding to the abscissas values

$$x_1, x_2, x_3, \dots, x_N, x_{N+1}, x_{N+2}, x_{N+3}, \dots, x_{2N}.$$

And the average of the elastic modulus of the rod-shaped object is obtained as

$$\bar{E}_1 = \frac{\sum_{k=1}^{2N} E_k}{2N} \quad (12)$$

The standard deviation of the elastic modulus of the rod-shaped object is obtained as

$$\delta = \left(\frac{1}{2N} \sum_{i=1}^{2N} (E_i - \bar{E})^2 \right)^{\frac{1}{2}} \quad (13)$$

According to the 3 times standard deviation criterion, the gross errors outside the range of $\bar{E}_1 - 3\delta \leq E \leq \bar{E}_1 + 3\delta$ should be removed. The T removed ones are expressed as $E_1^{(d)}, E_2^{(d)}, E_3^{(d)}, \dots, E_T^{(d)}$. Therefore the elastic modulus can be computed as

$$\bar{E} = \frac{\sum_{k=1}^{2N} E_k - \sum_{p=1}^T E_p^{(d)}}{2N - T} \quad (14)$$

The cross section moment of inertia of deflection difference can be expressed as

$$I = \frac{\pi D^4}{64} \quad (9)$$

where D is the equivalent diameter of the rod-shaped object.

If the both ends of the rod-shaped object are supported, the theoretical deflection curve can be expressed as

Algorithm 2: The ordinates corresponding to the abscissas $x_1, x_2, x_3, \dots, x_N, x_{N+1}, x_{N+2}, x_{N+3}, \dots, x_{2N}$ of the contour points are obtained by using image processing under the loading and no-loading conditions. The ordinates $G_i^{(UY2)}(x_i)$ ($i = 1, 2, 3, \dots, N, N+1, N+2, N+3, \dots, 2N$), $G_i^{(LY2)}(x_i)$ ($i = 1, 2, 3, \dots, N, N+1, N+2, N+3, \dots, 2N$) of the upper contour and lower contour points are extracted under loading condition. The ordinates $G_i^{(UY1)}(x_i)$ ($i = 1, 2, 3, \dots, N, N+1, N+2, N+3, \dots, 2N$), $G_i^{(LY1)}(x_i)$ ($i = 1, 2, 3, \dots, N, N+1, N+2, N+3, \dots, 2N$) of the upper contour and lower contour points are extracted under no-loading condition.

The corresponding deflection difference of the abscissas between loading and no-loading condition can be found by the following equation.

$$w_i(x_i) = \frac{G_i^{(UY2)}(x_i) + G_i^{(LY2)}(x_i)}{2} - \frac{G_i^{(UY1)}(x_i) + G_i^{(LY1)}(x_i)}{2} \quad (i = 1, 2, 3, \dots, N, N+1, N+2, N+3, \dots, 2N) \quad (15)$$

Based on Equation (15), $2N$ elastic modulus values $E_1, E_2, E_3, \dots, E_N, E_{N+1}, E_{N+2}, E_{N+3}, \dots, E_{2N}$ can be gotten corresponding to the abscissas values $x_1, x_2, x_3, \dots, x_N, x_{N+1}, x_{N+2}, x_{N+3}, \dots, x_{2N}$. The average value and the standard deviation of the elastic modulus of the rod-shaped object are obtained by using Equation (12) and Equation (13). According to the 3 times standard deviation criterion, the gross errors should be removed. The remaining elastic modulus value can be computed as using Equation (14).

Algorithm 3: The left half upper contour LU function $F_{LU1}(x)$ and the lower contour LL function

$F_{LL1}(x)$ under no-loading condition can be fitted and expressed as

$$F_{LU1}(x) = \sum_{k=0}^4 a_k x^k \quad (16)$$

$$F_{LL1}(x) = \sum_{k=0}^4 b_k x^k \quad (17)$$

where a_k and b_k are the coefficients of the fitted functions.

The right half upper contour RU function $F_{RU1}(x)$ and the lower contour RL function $F_{RL1}(x)$ under no-loading condition can be fitted and expressed as

$$F_{RU1}(x) = \sum_{k=0}^4 c_k x^k \quad (18)$$

$$F_{RL1}(x) = \sum_{k=0}^4 d_k x^k \quad (19)$$

where c_k and d_k are the coefficients of the fitted functions.

The left half upper contour LU function $F_{LU2}(x)$ and the lower contour LL function $F_{LL2}(x)$ under loading condition can be fitted and expressed as

$$F_{LU2}(x) = \sum_{k=0}^4 e_k x^k \quad (20)$$

$$F_{LL2}(x) = \sum_{k=0}^4 f_k x^k \quad (21)$$

where e_k and f_k are the coefficients of the fitted functions.

The right half upper contour RU function $F_{RU2}(x)$ and the lower contour RL function $F_{RL2}(x)$ under loading condition can be fitted and expressed as

$$F_{RU2}(x) = \sum_{k=0}^4 g_k x^k \quad (22)$$

$$F_{RL2}(x) = \sum_{k=0}^4 h_k x^k \quad (23)$$

where g_k and h_k are the coefficients of the fitted functions.

The curve LC and the curve RC under no-loading condition can be expressed as

$$F_{LC1}(x) = \frac{F_{LU1}(x) + F_{LL1}(x)}{2} \quad (24)$$

$$F_{RC1}(x) = \frac{F_{RU1}(x) + F_{RL1}(x)}{2} \quad (25)$$

The curve LC and the curve RC under loading condition can be expressed as

$$F_{LC2}(x) = \frac{F_{LU2}(x) + F_{LL2}(x)}{2} \quad (26)$$

$$F_{RC2}(x) = \frac{F_{RU2}(x) + F_{RL2}(x)}{2} \quad (27)$$

The deflection difference $w_1, w_2, w_3, \dots, w_N, w_{N+1}, w_{N+2}, w_{N+3}, \dots, w_{2N}$ for each $x_1, x_2, x_3, \dots, x_N, x_{N+1}, x_{N+2}, x_{N+3}, \dots, x_{2N}$ can be obtained using $F_{LC1}(x), F_{RC1}(x), F_{LC2}(x)$ and $F_{RC2}(x)$ between loading and no-loading conditions.

$$w_i(x_i) = F_{LC2}(x_i) - F_{LC1}(x_i) \quad (i=1, 2, \dots, N) \quad (28)$$

$$w_j(x_j) = F_{RC2}(x_j) - F_{RC1}(x_j) \quad \left(j = N+1, N+2, \dots, 2N \right) \quad (29)$$

The average values of the elastic modulus at the left half and right half of the rod-shaped object are obtained as

$$\bar{E}_1 = \frac{\sum_{k=1}^N E_k}{N} \quad (30)$$

$$\bar{E}_2 = \frac{\sum_{k=N+1}^{2N} E_k}{N} \quad (31)$$

The standard deviations of the elastic modulus at the left half and right half of the rod-shaped object are obtained as

$$\delta_1 = \left(\frac{1}{N} \sum_{i=1}^N (E_i - \bar{E}_1)^2 \right)^{\frac{1}{2}} \quad (32)$$

$$\delta_2 = \left(\frac{1}{N} \sum_{i=N+1}^{2N} (E_i - \bar{E}_2)^2 \right)^{\frac{1}{2}} \quad (33)$$

According to the 3 times standard deviation criterion, the gross errors should be removed. The R removed ones are expressed as $E_1^{(t)}, E_2^{(t)}, E_3^{(t)}, \dots, E_R^{(t)}$. Therefore the elastic modulus at the left half of the rod-shaped object can be computed as

$$\bar{E}_1 = \frac{\sum_{k=1}^N E_k - \sum_{p=1}^R E_p^{(t)}}{N - R} \quad (34)$$

According to the 3 times standard deviation criterion, the gross errors should be removed. The Q removed ones are expressed as $E_1^{(d)}, E_2^{(d)}, E_3^{(d)}, \dots, E_Q^{(d)}$. Therefore the elastic modulus at the right half of the rod-shaped object can be computed as

$$\bar{E}_2 = \frac{\sum_{k=N+1}^{2N} E_k - \sum_{p=1}^Q E_p^{(d)}}{N - Q} \quad (35)$$

The final elastic modulus can be expressed as

$$\bar{E} = \frac{\bar{E}_1 + \bar{E}_2}{2} \quad (36)$$

4 Experiment

The elastic modulus of a plant stem is measured to verify the proposed device and method. The vertical downward force shown in Fig.2 is 0.98N.

By using Algorithm 3, the elastic modulus at the left half of the plant stem are obtained as 14.153, 13.938, 13.820, 13.751, 13.709, 13.679, 13.656, 13.634, 13.612, 13.589, 13.566, 13.543, 13.523, 13.506, 13.495, 13.494, 13.505, 13.532, 13.580, 13.653 and 13.759 with the unit MPa. The elastic modulus at the right half of the plant stem are 11.262, 12.493, 13.129, 13.443, 13.585, 13.636, 13.644, 13.633, 13.620, 13.612, 13.613, 13.625, 13.647, 13.679, 13.719, 13.761, 13.804, 13.841, 13.867, 13.874 and 13.856 with the unit MPa.

5 Conclusions

A device and a method are proposed to measure the elastic modulus of the rod-shaped object based on image processing. The structure of the device is provided. The image of the rod-shaped object is gotten using the proposed measurement device. The coordinates of the point on the contour line and the centroid of the cross-section of the rod-shaped object are extracted by using the object image with loading and no-loading respectively. The elastic modulus is computed by using the deflection difference formula. Three computing algorithms are proposed and the corresponding formulae are given. Finally an example is given to verify the feasibility and effectiveness of the device and method that lay a solid foundation for future study of the rod-shaped object elastic modulus measurement.

Acknowledgments

This work is supported by Scientific and Technological Project of Henan Province of China with grant No. 172102310664. The authors would like to thank the anonymous reviewers for their valuable work.

References

1. Wang zheng, Gu Lingling, Gao Zizhen, and Lui Bin. Dynamic testing and probability distribution of elastic modulus of SPF dimension lumbers, *Scientia Silvae Sinicae*, **51**(2), 2015, 105-111.
2. Qi Yongfeng, Xu Huadong, and Wang Lihai. Comparative study on dynamic modulus of elasticity of wood using four different methods, *Forest Engineering*, **27**(1), 2011, 19-22.
3. Guo Yuanchen, and Wang Xue. Experimental research on elasticity modulus of recycled aggregate concrete, *Bulletin of the Chinese Ceramic Society*, **32**(3), 2013, 467-471.
4. Lui Hongbiao, and Li Hongnan, Evaluation method for material elastic modulus in the similitude design of structural shaking table test, *Journal of Vibration and shock*, **35**(3), 2016, 114-120.
5. Wan Detian, Bao Yiwang, Liu Xiaogen, and Tian Yuan. Elastic modulus evaluation technique and influencing factors analysis of glass materials, *Doors & windows*, **8**, 2012, 31-35.
6. Gao Zhihua, Wei Jiangbin, Zhang Cen, and Jia Yan. Measurement of metal elasticity modulus by strain gage, *Physics and Engineering*, **27**(2), 2017, 37-41+46.
7. Gustavo Marcati A Alves , Ronaldo D Mansano. Use of Protek-PSB as structural material for MEMS: measurement of elastic modulus, *Microelectronics Technology and Devices*, **31**, 2016, 1-4.
8. Ren Jie. Research on elastic modulus testing system based on ultrasonic, Nanjing University of Science and Technology, 2017.
9. Chen Cheng, Li Xianglian, Liu Weiwei, and Zhang Dongge. Design of measuring elasticity instrument of wire by using linear CCD, *Experimental Technology and Management*, **33**(1), 2016, 104-106.
10. Lwanaga Hiroshi, Okuyama Sadatoshi, Shimada Takahiro. Equipment for measuring high temperature elastic modulus. *Sumitomo Metals*, **50**(3), 85-87, 1998.
11. Xu Jiabin, Yuan Haigan, Wu Hongbin, Ou Chaozhao, and Zou Xiaoming. Improvement of measuring young's modulus by resonance method, *Physical experimentation*, **31**(11), 2011, 43-46.
12. Christophe Auvray, Noémie Lafrance, and Danièle Bartier. Elastic modulus of claystone evaluated by nano-/micro-indentation tests and meso-compression tests, *Journal of Rock Mechanics and Geotechnical Engineering*, **9**(1), 2017, 84-91.
13. Li Mingxiang. Laser interferometry measurements of Young's modulus of material, Northeast Normal University, 2015.
14. Chiu Chin-Chen, Case, Eldon D. Elastic modulus determination of coating layers as applied to layered ceramic composites. *Materials Science and Engineering A*, **132**, 39-47, 1991.
15. Niu Lianping. Studying two question in experiment of measuring elastic modulus by stretching method, *Journal of Luoyang Normal University*, **32**(2), 2013, 59-60.
16. Lui Hongwen, *Material mechanics* , Higher education press, Beijing, 2011.